

# Structural and Electrical Properties of Polymorphic Pentacene Thin Films

B. Stadlober<sup>\*a</sup>, V. Satzinger<sup>a</sup>, H. Maresch<sup>a</sup>, D. Somitsch<sup>b</sup>, A. Haase<sup>a</sup>, H. Pichler<sup>a</sup>, W. Rom<sup>a</sup> and G. Jakopic<sup>a</sup>

<sup>a</sup> JOANNEUM RESEARCH Forschungsgesellschaft mbH, Institute of Nanostructured Materials and Photonics, Franz-Pichler-Strasse 30, 8160 Weiz, Austria

<sup>b</sup> Karl-Franzens University Graz, Institute of Experimental Physics, Universitätsplatz 3, 8010 Graz, Austria

## ABSTRACT

Due to its outstanding carrier transport capabilities the aromatic hydrocarbon pentacene is still one of the most promising out of all organic semiconducting materials investigated so far. Pentacene appears in several polymorphic structures that significantly differ with respect to the d(001) spacing. It is shown, that precise control of the epitaxial growth process of thin films enables not only to adjust the formation of the polymorphic phases, but also to influence grain size and shape. The relative volume fraction of the pentacene polymorphs is determined by several parameters which are substrate material, deposition rate, film thickness and substrate temperature. A comparison of X-ray diffraction and Raman measurements reveals that the phase with the smaller layer-by-layer spacing grows on top of the other. Moreover, there is a strict correlation between evaporation rate and maximum grain size. In addition to structural we also investigated the electrical properties of pentacene thin films focussing on polymorphism and its influence on the transport properties. Apart from the fact that the charge carrier mobility is strongly influenced by the grain size it turned out that the bulk phase is related to a lower intrinsic mobility than the thin film phase.

**Keywords:** organic field effect transistors, polymorphs, organic dielectrics, mobility, Raman, X-ray, atomic force microscopy

## 1. INTRODUCTION

Due to the impressive progress of the performance of organic devices over the last decade it seems increasingly likely that organic electronics will be used in a number of low-cost and large area applications such as active-matrix flat-panel displays, smart cards, electronic paper, identification tags and large-area sensor arrays. Organic electronics is extraordinary compared to inorganic electronics for two reasons. On the one hand, it is possible to process the devices at much lower temperatures than used in standard semiconductor industry. This allows to integrate the electronic circuits on large-area, inexpensive, flexible, low-weight, durable and even biologic substrates which opens a wide field of novel applications. Among others these are body-integrated intelligent detectors and sensors, electronic wall paper and flexible displays. On the other hand, organic materials allow to apply new and unconventional structuring techniques, such as nanoimprinting. This enables a straightforward downscaling of the critical dimensions to the submicron regime.

The key element of organic electronics is the organic field-effect transistor. Over the last years many groups put a major effort into the improvement of the electrical input and output characteristics of organic field-effect transistors by variation of the dielectric material<sup>1-11,17</sup>, optimisation of the contact characteristics<sup>21-22</sup> and modification of the design<sup>1</sup> but only moderate effort was made to thoroughly control the evaporation and growth process of the active semiconducting layer<sup>7,15,18</sup>.

For pentacene, a linearly condensed aromatic hydrocarbon composed of five benzene rings, the situation is particularly complex. Similar to other organic materials it has a strong tendency to form weakly bound van-der-Waals molecular single crystals. During the growth process the molecules arrange in a herringbone structure within each elementary cell. Low-energy electron micrographs have shown that during the initial stages of growth stable two-dimensional islands nucleate on the surface of the substrate that avoid touching each other<sup>4</sup>. Each of these grains forms a randomly oriented pentacene single crystal with increasing grain sizes for very clean and also passivated surfaces<sup>4,16</sup>. It is well known, that pentacene thin films appear in several polymorphic structures, which differ significantly by the tilt of the longitudinal

---

\* [barbara.stadlober@joanneum.at](mailto:barbara.stadlober@joanneum.at); phone 0043-3172-603-2721; fax 0043-3172-603-2710

axis of the molecules to the substrate surface, respectively by the c-axis length of the corresponding elementary cell<sup>7,15,16,17,18</sup>. Since the transport properties strongly depend on the interaction of delocalised  $\pi$ -electron orbitals between adjacent molecules a decrease of the molecular tilt angle means a decrease of the orbital overlap of the neighbours and consequently one may expect a lower intrinsic mobility of the charge carriers. However, it is still unclear which parameters of the growth process, as for example evaporation rate, substrate temperature, vacuum condition or film thickness are critical with respect to the formation of a specific phase and if other factors such as the substrate material, its pretreatment and the degree of purity of the source material have a strong influence on the crystallization and growth process as well. Among all the substrate materials for pentacene thin film growth thermally generated silicon dioxide is the best investigated as it is commonly used for the dielectric layer in organic thin film transistors<sup>1,2,3,4,5,6,7</sup>. Only a few groups studied pentacene growth conditions on other inorganic dielectrics<sup>8,9,10,11</sup> and even less on organic compounds<sup>12,13,14</sup>. As there is no overall agreement on the relevant parameters for controlled phase formation, even the number of polymorphic phases is unclear<sup>18</sup>, the correlation of film structure and charge carrier mobility is not straightforward<sup>7,15,16,18</sup>.

It is the aim of this work to clarify these questions by extensive growth experiments and a detailed analysis of the relevant film quality parameters such as grain size and shape, ordering, roughness and polymorphism and their influence on the interesting electrical properties.

## 2. EXPERIMENTAL

For the electrical characterization common-gate thin film transistors in a top-contact configuration were fabricated with a layer sequence that already has been described in literature<sup>2,3</sup>. As dielectrics either inorganic (200-300nm thermally-grown SiO<sub>2</sub> on highly-doped silicon wafers from commercial sources) or organic materials (several polymer compounds such as polymethylmetacrylate (PMMA) and polyvinylphenol-copolymer (PVP) in suitable solutions deposited via spin-on process on gold-coated substrates) were used. On these substrates the epitaxially grown pentacene films were deposited by thermal evaporation under high-vacuum conditions in a standard configuration. We used high-purity pentacene from different sources. The source and drain electrodes were evaporated through shadow masks on top of the semiconducting layer to form 30-50nm thick gold contacts. Transistor test structures were fabricated with channel lengths ranging from 20-200 $\mu$ m and channel widths from 2000-3000 $\mu$ m. The X-ray diffraction (XRD) measurements were performed in Bragg-Brentano configuration in a Siemens standard diffractometer by using the Cu-K $\alpha$  radiation. The Raman measurements were done on a Dilor triple monochromator in backscattering geometry, which allows detecting Raman signals down to 20cm<sup>-1</sup> relative to the directly reflected laser line at 647nm.

## 3. STRUCTURAL CHARACTERIZATION

Characterization of epitaxially-grown pentacene thin films by atomic force microscopy (AFM) provides an insight into how different process and input parameters are correlated (Fig.1,2,3).

### 3.1 Substrate Material

In the thermodynamic limit the growth morphology is determined by the balance of the interfacial free energies involved. For substrate temperatures near room temperature thin films are grown far from thermodynamic equilibrium, the resulting morphology will then be governed by kinetic effects. If the interlayer mass transport is fast enough to allow atoms to leave the tops of growing 2D islands as soon as they arrive, the growing layer will be completed before second layer nucleation sets in and smooth layer-by-layer growth results<sup>23,24</sup>. If, however, interlayer mass transport is hindered by a sufficiently large diffusion barrier at the island edge, growth in the next layer starts before the previous one is filled and 3D structures develop (multilayer or 3D growth). In principle this model can be transferred to the growth of organic thin films. It has been shown<sup>4</sup>, that the nucleation density of the first crystalline molecular layer  $N_1$  is determined by the ratio of the growth rate  $R$  to  $D_s$ , which is the diffusion constant of pentacene on the substrate and by the presence of reactive sites at the surface. Nucleation of the second layer takes place when the islands in the first layer exceed a critical size  $L_c$ . If  $L_c$  is small compared with the separation between islands, meaning  $L_c^2 < 1/(\pi N_1)$ , islands will nucleate a second layer before coalescence, giving multilayer growth. The critical island size depends on  $R$ , on the diffusion constant  $D_p$  of pentacene on pentacene and on the height of the diffusion barrier at the island step-edge. Since the

diffusion constants are not identical the nucleation density critically depends on the substrate, whereas the critical island radius does not<sup>4</sup>. High evaporation rates and poorly controlled surfaces with a lot of reactive bonds result in enhanced 2D or layer-by-layer growth yielding densely packed, smooth pentacene films with small grains and a high grain-boundary density.

There is a number of substrate materials that, due to their specific physical interaction with the condensing molecules, are a good basis for the formation of polycrystalline films with high molecular ordering. In this case the topography of the films resembles a mountainous region composed of separated, dendritic shaped grains (Fig.1b-d). Although the branched shape of the crystallites is typical for pentacene films grown on thermal SiO<sub>2</sub> (Fig.1b), a very smooth substrate (RMS roughness = 0,3-0,4 nm), a lot of organic materials ranging from dielectric to conducting doped polymers also support the formation of overlapping, dendritic grains (Fig.1c,d). Here the RMS roughness is slightly smaller than for SiO<sub>2</sub> namely 0,24-0,38 nm for PMMA and 0,25-0,29 nm for PVP. The peak-to-valley roughness of the pentacene layer is in the order of the film thickness *d*, meaning that the growth dynamics along the direction perpendicular to the substrate plane is enhanced with respect to that in plane. This is what we expect for 3D island or multilayer growth.

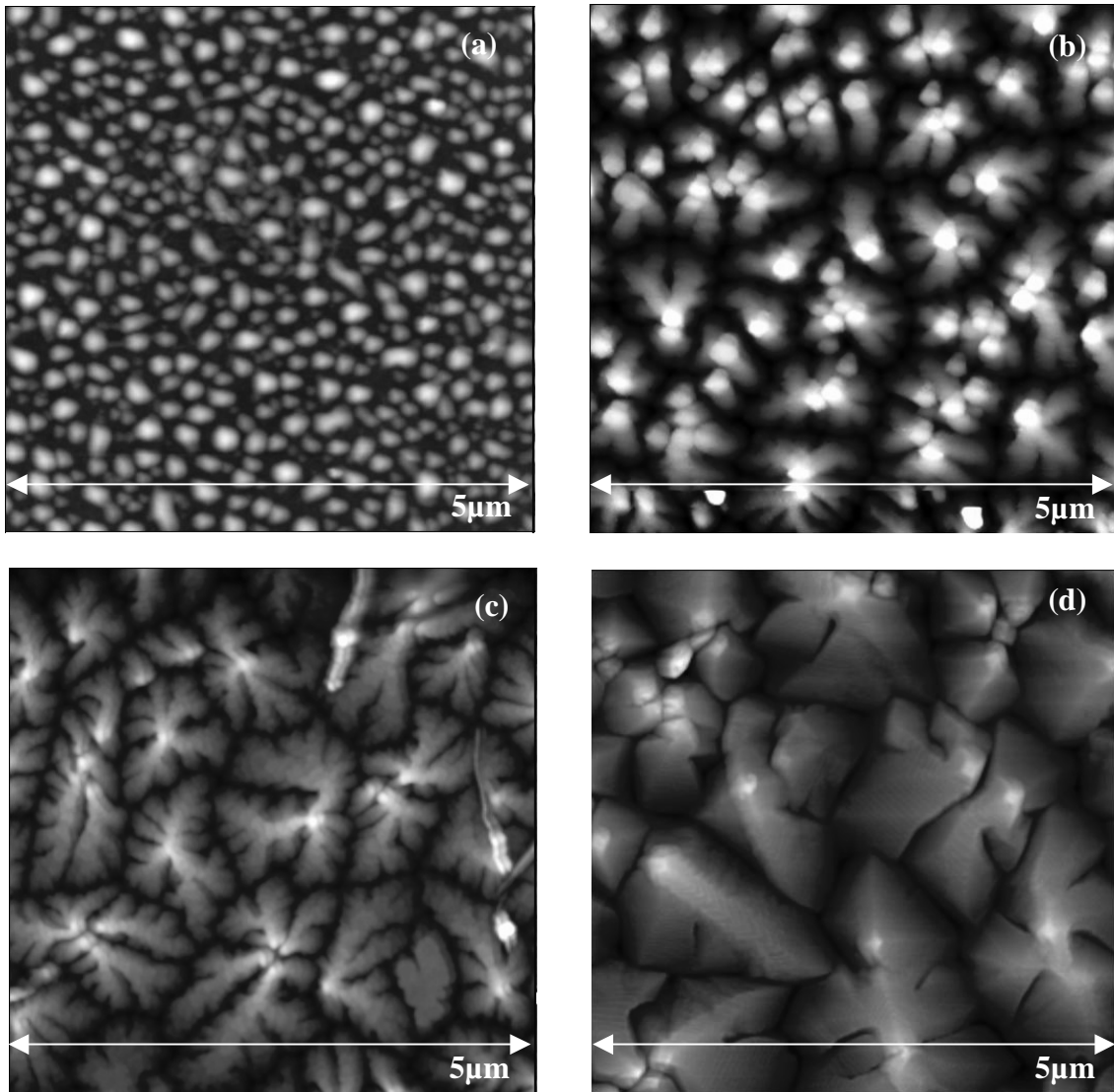


Figure 1: Atomic force microscopy (AFM) images of thermally evaporated pentacene films (*d*=50nm) on different dielectrics: (a) glass slide  $s_{av}$ =0,2µm, (b) thermal SiO<sub>2</sub>  $s_{av}$ = 1,1µm, (c) spin coated PMMA  $s_{av}$ =1,7µm, (d) spin coated PVP  $s_{av}$ = 2,6µm. Here  $s_{av}$  indicates the average grain size that can be deduced from the images.

The pentacene films shown in Fig.1 were all deposited at the same substrate temperature (25°C), the same nominal deposition rate ( $R \sim 1\text{nm}/\text{min}$ ) by using the same source material resulting in the same nominal film thickness. Comparing the AFM images with respect to the grain size reveals that the average grain size increases in going from  $\text{SiO}_2$  to polymer substrates which is due to a decreasing nucleation density in the early stages of the 3D island growth process. However, this can at best be assessed as a tendency, because there are a lot of other parameters that also influence the grain size, as for instance substrate temperature and evaporation rate (see below).

In many of the organic substrate materials the adsorbate-substrate interaction is stronger than in  $\text{SiO}_2$  leading to a better adhesion of the organic layer. This can be concluded from the thermal desorption behavior. If the substrate is heated during the coating process then the number of desorbing molecules increases, compared to room temperature. The temperature at which the number of adsorbing and desorbing molecules is equal, meaning that no film adheres to the substrate, is significantly higher for polymers than for  $\text{SiO}_2$ . It is not reasonable to give absolute numbers, because the thermal desorption temperature is a sensitive parameter of the pressure conditions in the preparation chamber, the geometric setup of the coating block (distance and angle between evaporation cell and substrate) and all relevant parameters of the evaporation process itself. The observation of increasing interaction between substrate and condensed material for polymer substrates (especially PVP) leading to a decreased diffusion constant  $D_s$  is conflicting with the observation of decreased nucleation density for these materials corresponding to larger grains in subsequent stages of growth. Therefore we conclude that for growth in high-vacuum conditions it is predominantly the cleanliness of the substrate surface and the slightly smaller roughness that controls the initial nucleation density.

If pentacene molecules condense on glass substrates homogenous films composed of tiny, elliptically shaped grains are formed (Fig.1a). In this case the roughness of the film is one order of magnitude lower than its thickness meaning that the growth mode is dominantly layer-by-layer due to a much higher nucleation density in the initial stages of growth.

### 3.2 Substrate Temperature

An increase of the substrate temperature during the condensation process usually leads to an increase in the average and the maximum grain size (Fig.2a,b). This is due to the fact that for higher temperatures the mobility of molecules arriving at the surface is increased resulting in a better alignment of the molecules and a lower nucleation density (see above). However, the correlation between substrate temperature and grain size is not clear because other processes are also influenced by temperature. Thermal desorption plays a role together with temperature-induced phase transformation processes<sup>18</sup> and changes in the volume fraction of the different pentacene phases<sup>7</sup>. This latter effect may be the reason for the differences in grain size and shape observed for the film deposited at 75°C (Fig.2c) compared to the one at 65°C. At 75°C the crystallites are rather square and obviously smaller than for the deposition at 65°C. In order to separate the different processes influencing the film formation it is necessary to vary independent parameters only. Therefore the substrate temperature was kept constant at 25°C throughout most experiments.

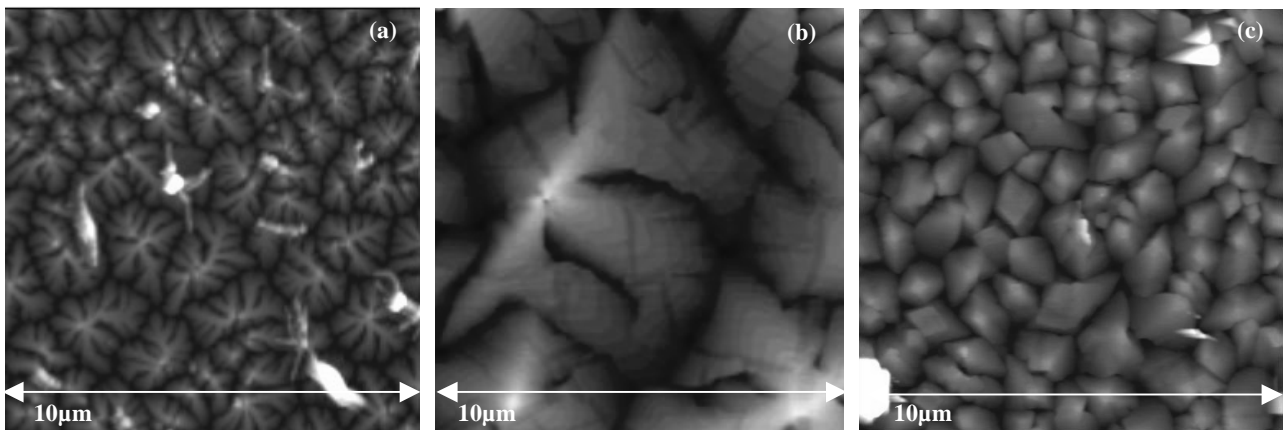


Figure 2: Atomic force microscopy images of pentacene films ( $d=50\text{nm}$ ) evaporated on thermal  $\text{SiO}_2$  at different temperatures and for  $R=1\text{nm}/\text{min}$ : (a) 25°C (b) 65°C (c) 75°C

### 3.4 Deposition Rate

In Fig.3 the influence of a reduction of the deposition rate is illustrated. All films are about 50nm thick and were grown at room temperature on the same SiO<sub>2</sub> substrate as in the other experiments. It is clearly visible that decreasing the deposition rate not only increases the grain size but also changes the surface morphology of the films from an assembly of squared grains to one of dendritic grains. Due to the fact that for sub-monolayer coverages the islands are two-dimensional, whereas for larger coverages they transform into 3D islands depending on the substrate material and substrate cleanliness<sup>4,16</sup>, it is preliminary the deposition rate at the initial stages of the nucleation process that determines the nucleation density (see above) for a given substrate material and a given temperature. As will be shown later the phase formation is also strongly influenced by the molecular flux density. For a control of the growth process, it is inevitable to precisely adjust the deposition rate.

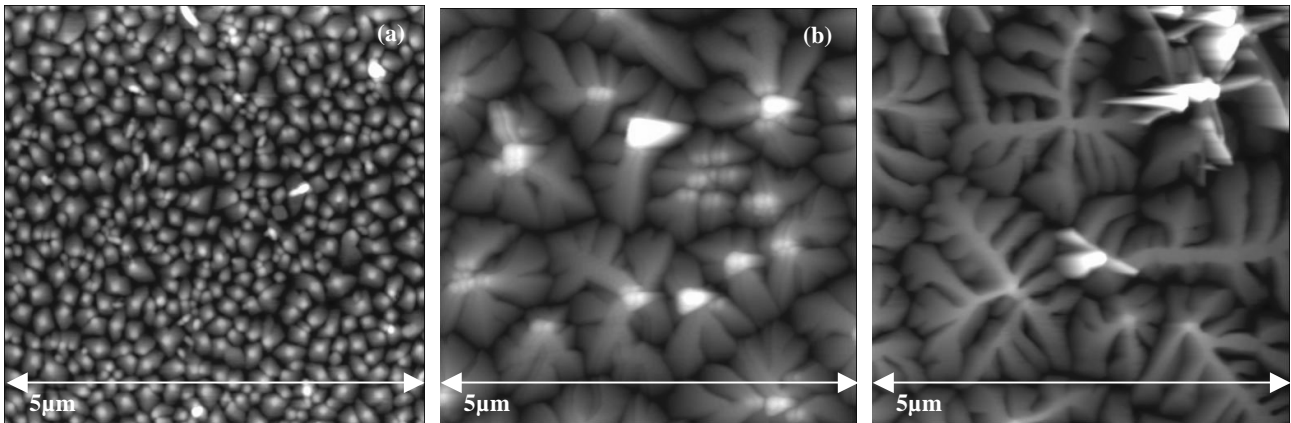


Figure 3: Comparison of atomic force microscopy images of pentacene thin films on silicon dioxide deposited at different initial rates (a) 6nm/min, (b) 1,1 nm/min, (c) 0,4 nm/min

In all experiments initially the deposition rate was kept constant at a specific value but in some cases was increased later on. The correlation of the initial deposition rate with the maximum grain size is shown in Fig.4a and compared to the respective correlation for average deposition rates in Fig.4b.

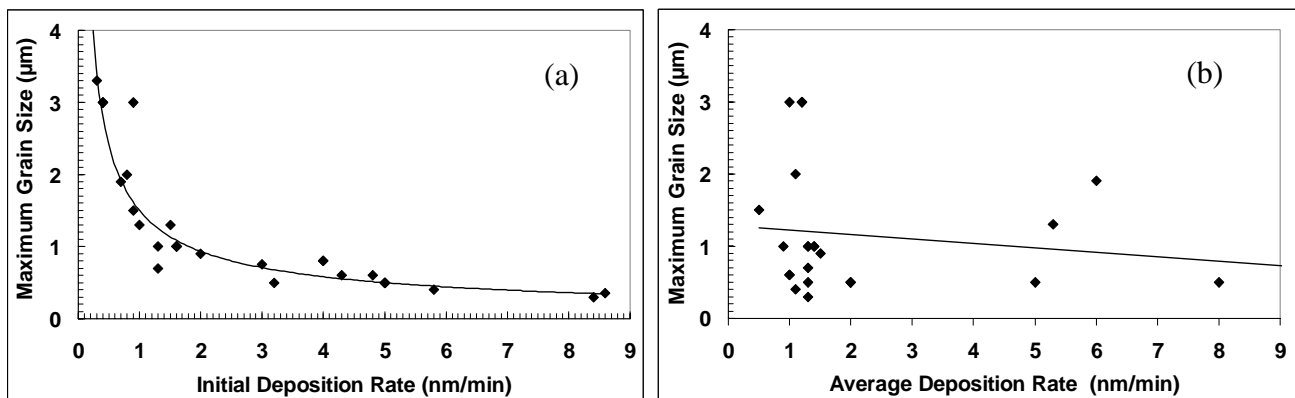


Figure 4: Correlation between maximum grain size and deposition rate for pentacene thin films on thermal SiO<sub>2</sub> for (a) initial deposition rate, (b) average deposition rate

It is obvious that the maximum grain size shows a potential-law dependence on the initial deposition rate, whereas there is almost no correlation to the average deposition rate. Similar correlations between grain size and deposition rate exist for polymer substrates (for instance PMMA). This difference in the parameter extraction may explain why some groups see a correlation between deposition rate and grain size<sup>7,8,16</sup>, while others do not<sup>15</sup>.

### 3. Polymorphs of Pentacene

X-ray diffraction patterns have shown that, depending on the growth conditions, pentacene crystallizes in several structural phases that differ by their layer-by-layer spacing. In Fig.5 the first-order diffraction peak of two thin films is compared to crystalline powder from a grinded single crystal.

The film deposited at the lower rate shows two peaks, one at  $5,7^\circ$  corresponding to a lattice spacing of  $15,5\text{\AA}$  and a tilt of the molecules of about  $17^\circ$  to the surface normal. In literature this phase is called “thin-film phase”. The second peak is at  $6,1^\circ$  which corresponds to a layer-by-layer spacing of  $14,5\text{\AA}$  and a tilt of the c-axis of the molecules to the surface normal of  $25,7^\circ$  and is very close to the (001)-peak of the single crystal phase at  $6,25^\circ$  that corresponds to a tilt of  $28^\circ$ . The respective phase is commonly referred to as the “bulk phase”. If one accounts for the change in the volume fraction of the two-phase system (thin film and bulk phase) with respect to the deposition rate it turned out that the portion of the bulk phase increases with increasing deposition rate.

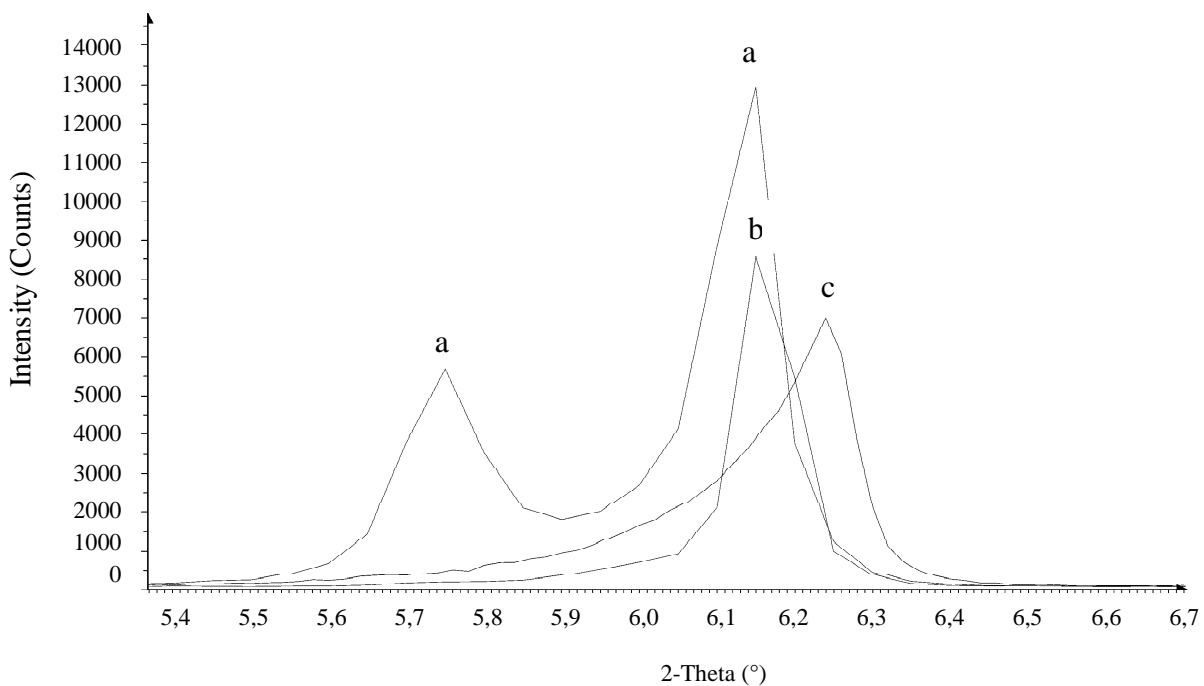


Figure 5: (001)-reflex of the XRD pattern from different pentacene samples: (a) thin film deposited on  $\text{SiO}_2$  at a deposition rate of  $R \sim 1,5\text{nm/min}$ , (b) thin film deposited on  $\text{SiO}_2$  at  $R \sim 6\text{nm/min}$  and (c) grinded single crystal.

A substantial contribution of the thin-film phase to the overall volume can be expected only for deposition rates  $R < 1\text{nm/min}$ <sup>19</sup>. Note that both phases in this two-phase system are crystalline and highly ordered.

Concerning the morphology, atomic force microscopy images reveal that the film with the higher deposition rate shows approximately squared grains, whereas the one with the lower deposition rate consists of dendritic grains. Therefore one may conclude that the bulk phase corresponds to the squared grains and the thin film phase to the dendritic ones. It has been reported<sup>7,18</sup> that higher substrate temperatures result in an increase of the volume fraction of the bulk phase at the expense of the thin film phase. Comparing this with the evolution of the shape of the grains from Fig.2 by increasing the substrate temperature also supports the assignment of squared grains to the bulk and dendritic grains to the thin film phase. For a final clarification of this question a larger group of samples has to be investigated by X-ray diffraction.

### 3.6 Film thickness

The film thickness  $d$  is another important parameter that is related to the formation of the two-phase system. As Fig.6 demonstrates, even for very low deposition rates ( $\ll 1\text{nm/min}$ ) where the formation of the bulk phase should be suppressed or at least retarded (see below), a small contribution of the bulk phase arises for  $d > 150\text{nm}$ . The volume fraction of the bulk phase increases with increasing film thickness. This corresponds to the observation of approximately squared grains in AFM images of the 300nm film.

Similar variations of the phase ratios with  $d$  have been observed for much higher evaporation rates<sup>7,18</sup>. The critical film thickness at which the contribution from the bulk phase becomes visible in the XRD ( $>2\%$ ) is pushed to lower critical film thickness values for higher deposition rates. Apart from the fact that the relative volume fraction of the two-phase system depends on the duration of the evaporation process (assuming constant rates), it is interesting to note that the width of the (001) reflex, that corresponds to the thin film phase, continuously gets smaller with increasing  $d$ . This clearly indicates an increase of the volume of the ordered scattering regions, which may either be due to an increase of the lateral grain size having not been observed by AFM or due to an increase of the vertical grain dimension. This latter assumption fits to a 3D island growth mode, which has a strong preference for growth perpendicular to the substrate compared to growth in lateral dimensions.

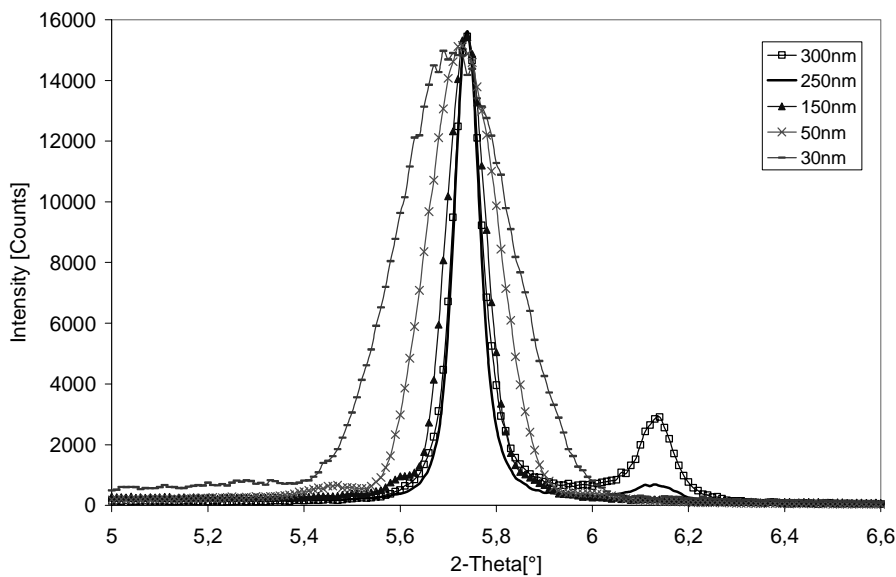


Figure 6: Comparison of the (001) reflex for pentacene films with different layer thickness values. The substrate dielectric is PMMA. The peak at about  $2\theta=5,7^\circ$  corresponds to the thin film phase, whereas the one at  $6,15^\circ$  belongs to the bulk phase.

Apart from the XRD experiments valuable information about polymorphism in pentacene can also be obtained from Raman measurements. In Fig.7 the low-frequency parts of Raman spectra from films with different  $d$ -spacings are compared. From a factor group analysis based on a triclinic elementary cell containing two molecules on non-equivalent symmetry sites six Raman active phonons with  $A_g$ -symmetry can be expected. The eigenfrequencies of the lattice modes are characteristic for a specific microscopic structure meaning that a difference in the tilt of the molecular axis to the substrate may result in a shift of the eigenfrequencies of the related lattice modes.

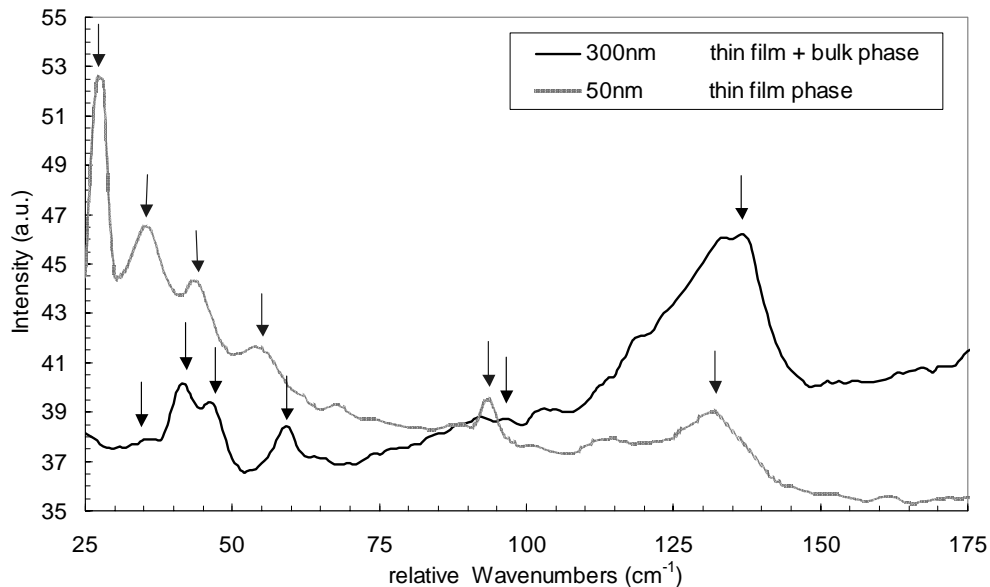


Figure 7: Raman spectra of pentacene thin films on PMMA with different layer thickness values recorded at 78K. The arrows indicate the phonons. The phase assignment is related to the XRD data.

In the spectrum of the 50nm film the six Raman lines can be identified as lattice phonons. These lines are marked with arrows and are attributed to the lattice vibrations of the thin film phase. Six structures (marked with arrows) are observed in the spectrum of the 300nm film too, although some of them are broadened with respect to the ones of the thin film phase. The lattice modes in the Raman spectrum of the 300 nm film are shifted towards higher frequencies by about  $3\text{-}7\text{ cm}^{-1}$  with respect to the peaks of the 50 nm film indicating another phase. Recalling the XRD results, these new lines can be attributed to the bulk phase. It is interesting to note that most of the thin-film modes are strongly suppressed in the 300nm spectrum, although the volume fraction of the bulk phase is only 20%. Raman is a surface sensitive method; the volume of the scattering region is determined by the optical penetration depth, which from ellipsometry turned out to be about 100 nm corresponding to a Raman probing depth of approximately 50 nm. Since no contribution of the thin film phase is observed it can be concluded that the bulk phase forms on top of the thin film phase with a layer thickness of at least 50 nm for the example discussed above. This is consistent with the second peak observed in the XRD pattern of the 250 nm sample in Fig.6 which corresponds to a 5% contribution of the bulk phase to the overall pentacene volume.

#### 4. Electrical Characterization

With regard to device applications the key question is how the different pentacene morphologies and phases differ with respect to their charge carrier transport properties and, most important, what are the mobility values to be assigned to the different phases. Therefore we investigated the electrical properties of a large number of thin-film transistors, that were constructed in the common-gate configuration with source and drain on top. In this work only those results will be presented that are directly related to the dependence of the carrier mobility on the film thickness.

There are several transistor parameters that can be deduced from the input and output measurements representing a characteristic fingerprint of the device. These parameters are the threshold voltage, the on/off ratio, the leakage currents, the subthreshold slope, the breakdown voltage of the dielectric (dielectric strength), the hysteresis and last but not least the charge carrier mobility  $\mu$ . It is this parameter that tells us the most about the transport mechanisms, although a complete understanding of the transport dynamics is possible only by taking into account all parameters<sup>19</sup>.

In the following, only the charge carrier mobility in the saturation regime, which seems to be the most relevant one for applications in logic circuits, will be discussed. The mobility in the linear regime shows a similar behavior but in most cases is smaller.

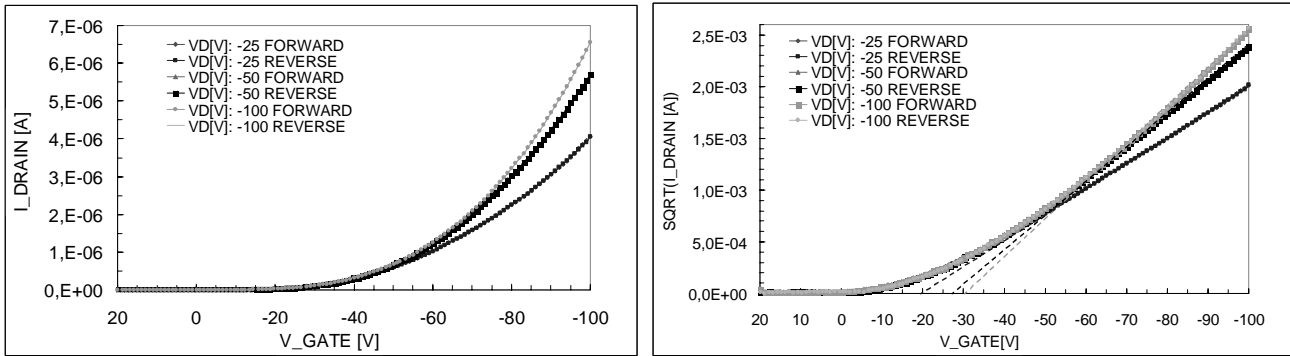


Figure 8: Input characteristics of an organic thin-film transistor with 50nm pentacene as active semiconducting layer and 1 $\mu$ m PMMA as dielectric layer. The left diagram corresponds to the same data, but here the square root of the drain current vs. gate voltage is plotted.

Under the assumption of  $\mu$ =constant the saturation field-effect mobility can be extracted by either fitting a trendline to the high-voltage region of the square-root of the input characteristics (plotting the square root of the drain current against the gate-voltage) or by differentiating the square root of the drain current with respect to the gate voltage. In Fig.8 the transfer characteristics of a pentacene thin film transistor with PMMA as the insulating layer is plotted. No hysteresis is observed, i.e. the dynamics for trapping and detrapping is very similar. The left diagram reveals that the saturation current approximately follows the quadratic law that is expected from a phenomenologic description of organic thin-film transistors working in accumulation<sup>20</sup>. It is interesting to note that not only the threshold voltage  $V_0$ , which is determined by the intercept of the trendline with the abscissa, is decreasing with decreasing drain voltage but also the slope. This indicates that the mobility is not only depending on the gate<sup>21</sup> but also on the drain voltage.

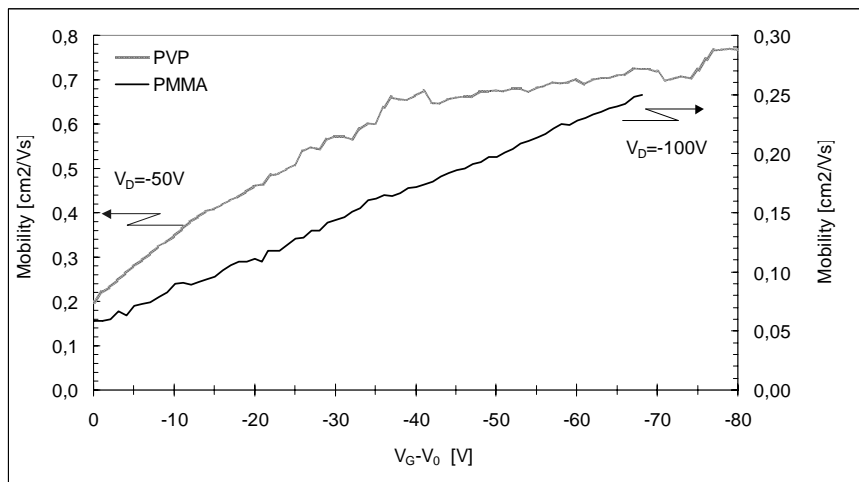


Figure 9: Gate voltage dependence of the mobility for pentacene thin film transistors with PMMA (red curve) and PVP (blue curve) as insulator. The gate voltage axis is corrected for the threshold voltage  $V_0$ .

The gate voltage dependence of the mobility of this sample is shown in Fig. 9 and compared to the one of a sample with 400nm PVP as dielectric layer. The PMMA transistor shows a linear increase of the mobility over the whole gate voltage sweep, whereas the PVP sample shows saturation at higher gate voltages. The linear increase in the mobility can be attributed to the effect that by increasing the upbending of the band edge with respect to the Fermi level more and more traps are filled within the bandgap. However, filled traps do not act as scattering centres for the charge carriers anymore. The mobility reaches its maximum value as soon as the lowest trap level (w.r.t. the valence band) is filled, a situation

that is referred to as the trap-filled limit. For higher gate voltages  $\mu$  is expected to stay constant as long as no other effects such as surface scattering or limiting by contact resistance effects occurs. For the PVP transistor the trap-filled limit mobility  $\mu_{TFL}$  which is close to the intrinsic mobility in the presence of filled traps is about  $0,8 \text{ cm}^2/\text{Vs}$  for  $V_D=-50\text{V}$ , whereas the maximum mobility of  $0,25 \text{ cm}^2/\text{Vs}$  for PMMA ( $V_D=-100\text{V}$ ) has to be regarded as a lower limit only. Here the trap filled limit is not reached yet. The interpretation of the drain voltage dependence of  $\mu_{TFL}$ , meaning that  $\mu_{TFL}$  increases with increasing drain voltage, is not that straightforward, but might be related to the increased pinching of the channel and the fact that the current path is probing less of the disturbed interface area.

Comparing the as extracted saturation field-effect mobilities with the size of the crystallites leads to a surprising correlation (Fig.10). If the pentacene layer of a transistor consists of grains with average size below  $1\mu\text{m}$  then the mobility is very low ( $\sim 10^{-2} \text{ cm}^2/\text{Vs}$ ). For polycrystalline films with grains of  $1\mu\text{m}$  one observes a steep increase in the mobility, which levels for larger crystallites. Such a threshold behavior can be expected if the carrier mean free path is about  $1\mu\text{m}$  resulting in increased surface scattering and grain boundary effects for fine granular layers. Above this threshold an increase in grain size does not drastically increase the mobility (about a factor of 2-3). A similar correlation is observed for PMMA. The mobility of the transistors investigated in this work can easily be increased by a factor of at least 2 by raising the substrate temperature to the desorption limit, which yields substantially larger grains.

A significant dependence of the mobility is also observed for variations in the pentacene layer thickness. In Fig.11 for each thickness value the average mobility is shown that is extracted from a group of devices. Up to  $150 \text{ nm}$  the mobility is approximately the same, meaning that this value is related to the thin film phase. For thicker films the mobility drops

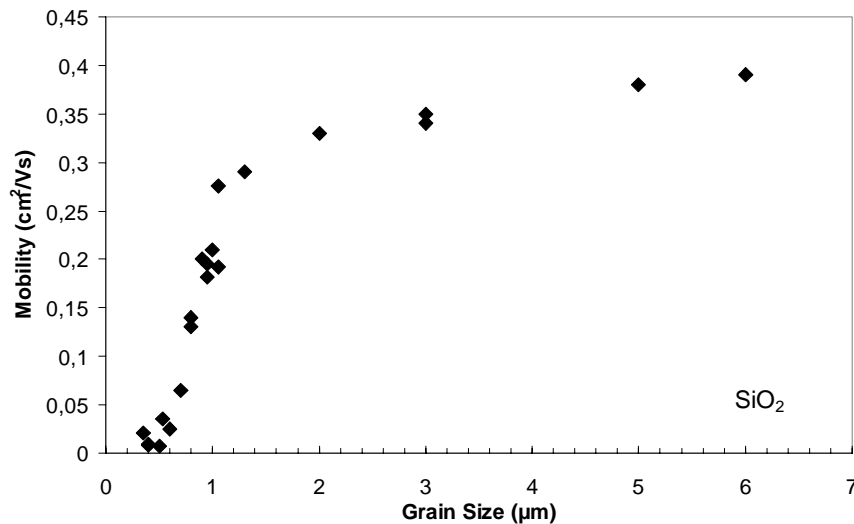


Figure 10: Correlation between mobility and grain size for pentacene films deposited on the gate dielectric  $\text{SiO}_2$ . The layer thickness ( $50 \text{ nm}$ ) and the substrate temperature ( $300\text{K}$ ) were kept constant throughout the series. The grain size was adjusted by varying the deposition rate.

to lower values, which could be either due to a substantial contribution of the bulk phase that is assumed to have a lower intrinsic mobility or to the fact that the contact resistance was higher.

Gold diffuses very easily through organic compounds resulting in a partly buried contact. For thick films the decreasing concentration of gold in the layer far from the surface may increase the contact resistance, decrease the current and correspondingly the mobility. The diffusion seems to stop at the second interface (the semiconductor-insulator interface). However, if the contact resistance limits the drain current level one would expect to see a continuous rather than a sudden decrease of the mobility with layer thickness. Therefore we believe that the bulk phase is characterized by an intrinsic mobility that is at least a factor of 2 smaller than the one of the thin film phase. A similar behavior is observed for  $\text{SiO}_2$  gate insulators and substrates.

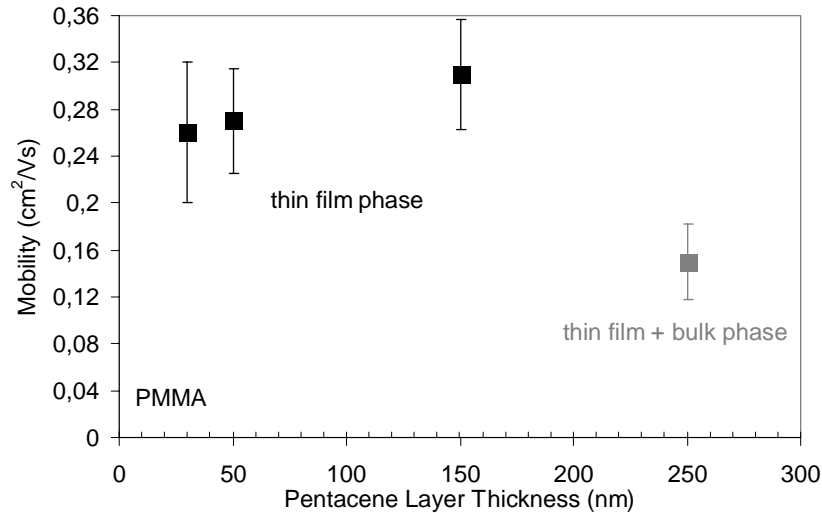


Figure 11: Dependence of the field effect mobility on the thickness of the active pentacene layer in organic thin film transistors based on a PMMA gate insulator. The error bars account for the standard deviation within a group of 3-7 transistors.

## 5. CONCLUSIONS

We have shown that precise control of the growth process and the growth conditions of pentacene thin films via adjusting the parameters substrate material, substrate temperature, deposition rate and film thickness result in films with specific granularity (grain size), surface morphology and phase distribution. The growth mode is a multiplayer (3D) island growth mode for substrates that are sufficiently inert to the arriving molecules. By decreasing the deposition rate the maximum grain size increases, following a potential law with the grains becoming more dendritic. Moreover, the volume fraction of the thin film phase, where the molecules form the largest angle to the substrate, increases with respect to the one of the bulk phase. This is true for all types of substrates used in this work ( $\text{SiO}_2$ , PMMA, PVP). However, by increasing the growth duration even for very low deposition rates the bulk phase starts to grow on the thin film islands above a critical film thickness value, what we can conclude from a comparison of the XRD and the Raman experiments. This critical film thickness is the higher the lower the deposition rate and the lower the substrate temperature is, a fact that was observed for all substrate materials investigated in this work. Increasing the substrate temperature results in larger squared grains, but also assists the formation of the bulk phase. The electrical characterization of the films by measuring the transfer characteristics of pentacene-based thin-film transistors indicated that the dependence of the mobility on the grain size shows a threshold behavior revealing a mean free path of  $1\mu\text{m}$  for the charge carriers. The mobility in the saturation regime is strongly gate-voltage dependent, a fact that can be attributed to the trapping of carriers during the gate voltage sweep. Depending on the quality of the semiconductor-insulator interface the trap-filled limit mobility, which is closely related to the intrinsic mobility, can be deduced from the characteristics. Furthermore it turns out that for various substrates the charge carrier mobility drops for transistors based on thick pentacene layers, which is attributed to the worse transport properties of the bulk phase. For the PVP insulator we observed a trap-filled limit mobility of about  $0,8\text{ cm}^2/\text{Vs}$  (for an operation voltage of  $V_D=-50\text{V}$ ), a value that can be doubled by increasing the substrate temperature.

## ACKNOWLEDGMENTS

The authors thank G. Leising, A. Fian, H. Schön, B. Lamprecht and M. Beutl for many helpful discussions and K. Pernstich for providing purified material.

## REFERENCES

- <sup>1</sup>H. Klauk, D.J. Grundlach, J.A. Nichols, C.D. Sheraw, M. Bonse, T.N. Jackson, "Pentacene Organic Thin-Film Transistors and ICs", *Solid State Technology*, **43**, 63-77, 2000; H. Klauk, M. Halik, U. Zschieschang, F. Eder, G. Schmid, and C. Dehm, "Pentacene organic transistors and ring oscillators on glass and on flexible polymeric substrates", *Appl. Phys. Lett.*, **82**, 4175-4177, 2003
- <sup>2</sup>I. Kyymissis, C.D. Dimitrakopoulos and S. Purushothaman, "Patterning pentacene organic thin film transistors", *J. Vac. Sci. Technol. B*, **20**, 956-959, 2000
- <sup>3</sup>S.F. Nelson, Y.-Y. Lin, D. J. Grundlach and T. N. Jackson, "Temperature-independent transport in high-mobility pentacene transistors", *Appl. Phys. Lett.*, **72**, 1854-1856, 1998
- <sup>4</sup>Frank-J. Meyer zu Heringdorf, M. C. Reuter and R. M. Tromp, "Growth dynamics of pentacene thin films", *Nature*, **412**, 517-520, 2001
- <sup>5</sup>Y.S. Yang, S. H. Kim, J-I Lee, H.Y. Chu, Lee-Mi Do, H. Lee, J. Oh, T. Zyung, M. K. Rye, and M.S. Jang, "Deep-level defect characteristics in pentacene organic thin films", *Appl. Phys. Lett.*, **80**, 1595-1597, 2002
- <sup>6</sup>W. A. Schoonveldt, J. Wildeman, D. Fichou, P.A. Bobbert, B. J. Van Wees, and T. M. Klapwijk, "Coulomb-blockade transport in single-crystal organic thin-film transistors", *Nature*, **404**, 977-980 (2000)
- <sup>7</sup>D. M. Knipp, R. A. Street, A. Völkel, and J. Ho, "Pentacene thin film transistors on inorganic dielectrics: Morphology, structural properties, and electronic transport", *J. Appl. Phys.*, **93**, 347-355 (2003)
- <sup>8</sup>C. D. Dimitrakopoulos, A. R. Brown, and A. Pomp, "Molecular beam deposited thin films of pentacene for organic field effect transistor applications", *J. Appl. Phys.*, **80**, 2501-2508, 1996
- <sup>9</sup>M. L. Swiggers, G. Xia, J. D. Slinker, A.A. Gorodetsky, G.G. Malliaras, R. L. Headrick, B. T. Weslowski, R. N. Shashidar, and C. S. Dulcey, "Orientation of pentacene films using surface alignment layers and its influence on thin-film transistor characteristics", *Appl. Phys. Lett.*, **79**, 1300-1302, 2001
- <sup>10</sup>M. H. Choo, W. S. Hong, and S. Im, "Characterization of pentacene organic thin film transistors fabricated on SiNx films by non-photolithographic processes", *Thin Solid Films*, **420-421**, 492-496, 2002
- <sup>11</sup>C.D. Dimitrakopoulos, S. Prurshothaman, J. Kyymissis, A. Callegari, and J. M. Shaw, "Low-voltage organic transistors on plastic comprising high-dielectric constant gate insulators", *Science*, **283**, 1999
- <sup>12</sup>H. Klauk, M. Halik, U. Zschieschang, G. Schmid, W. Radlik, and W. Weber, "High-mobility polymer gate dielectric pentacene thin film transistors", *J. Appl. Phys.*, **92**, 5259-5263, 2002
- <sup>13</sup>Z. Bao, V. Kuck, J.A. Rogers and M. A. Paczkowski, "Silesquioxane resins as high-performance solution processible dielectric materials for organic transistor applications", *Adv. Funct. Mater.*, **12**, 526-531, 2002
- <sup>14</sup>C. D. Sheraw, D. J. Grundlach, and T. N. Jackson, "Spin-on polymer gate dielectric for high performance organic thin film transistors", *Mat. Res. Soc. Symp. Proc.*, **558**, 403-408, 2000
- <sup>15</sup>M. Münch, "Strukturelle Beeinflussung der elektrischen Transporteigenschaften dünner organischer Schichten", *Dissertation*, Stuttgart 2001
- <sup>16</sup>A. Schoonveldt, "Transistors based on ordered organic semiconductors", *Dissertation*, Groningen 1999
- <sup>17</sup>C.D. Dimitrakopoulos and D.J. Mascaro, "Organic thin-film transistors: A review of recent advances", *IBM J. Res. & Dev.*, **45**, 11-27, 2001
- <sup>18</sup>C. C. Mattheus, A. B. Dros, J. Baas, G. T. Oostergetel, A. Meetsma, J. L. de Boer and T. T. M. Palstra, "Identification of polymorphs of pentacene", *Synthetic Metals*, 2002
- <sup>19</sup>B. Stadlober et al., to be published
- <sup>20</sup>G. Horowitz, R. Hajlaoui and H. Bouchriha, "The concept of "Threshold Voltage" in organic field-effect transistors", *Adv. Mater.*, **12**, 923-927, 1998
- <sup>21</sup>P. V. Necliudov, M. S. Shur, D. J. Grundlach, and T. N. Jackson, "Contact resistance extraction in pentacene thin film transistors", *Solid State Electronics*, **3200**, 2002
- <sup>22</sup>D. J. Grundlach and T. N. Jackson, "Pentacene TFT with improved linear region characteristics using chemically modified source and drain electrodes", *IEEE Electron Device Letters*, **22**, 571-573, 2001
- <sup>23</sup>K. Bromann, Harald Brune, H. Röder and K. Kern, "Interlayer Mass Transport in Homoepitaxial and Heteroepitaxial Metal Growth", *Phys. Rev. Lett.*, **75**, 677-680, 1995
- <sup>24</sup>J. Tersoff, A.W. Dernier van der Gon, and R. M. Tromp, "Critical Island Size For Layer-by-Layer Growth", *Phys. Rev. Lett.*, **72**, 266-269 (1994)